Computational Modelling Study of a Plane Gas Jet Impinging onto a Liquid Pool

S.E. Forrester and G.M. Evans
Department of Chemical Engineering
University of Newcastle, NSW 2308, AUSTRALIA

ABSTRACT

A plane turbulent gas jet impinging vertically onto a liquid pool has been successfully modelled using the computational fluid dynamics package CFX-F3D. This method allows the simultaneous evaluation of the gas flow field, the free liquid surface and the bulk liquid flow. Three different modes of surface deformation were investigated, namely dimpling, splashing and penetrating. The resulting characteristics of the cavity formed on the free liquid surface in each case, compared well with experimental and theoretical literature data. In particular, useful insight to the highly complex, and industrially relevant, penetrating mode has been achieved.

NOMENCLATURE

C	clearance between nozzle exit and undisturbed liquid surface	[m]
d_C	cavity diameter	[m]
g	gravitational acceleration	[m s^{-2}]
h_C	cavity depth	[m]
h_{DS}	cavity depth at the transition from dimpling to splashing	[m]
h_L	lip height	[m]
H	undisturbed liquid height in the receiving pool	[m]
K	constant in the centreline gas velocity eq.(1)	[-]
L_N	plane nozzle length	[m]
M	gas jet momentum	[N]
U_{CL}	centre-line gas velocity	[m s^{-1}]
U_N	gas velocity exiting nozzle	[m s^{-1}]
W_N	plane nozzle width	[m]
z	axial co-ordinate measured from nozzle exit	[m]
α	constant in eq.(3)	[-]
α_1, α_2	constants in eq.(4)	[-]
μ_L	liquid viscosity	[kg m^{-1} s^{-1}]
ρ_G	gas density	[kg m^{-3}]
ρ_L	liquid density	[kg m^{-3}]
σ	surface tension	[N m^{-1}]

1. INTRODUCTION

Gas jets impinging onto a pool of liquid are commonly encountered in the metallurgical industry as a method of agitating a molten liquid phase, *e.g.* oxygen steel making, vacuum degassing, argon-agitated ladles and top-blown copper converting. The gas jet causes a depression to be formed on the liquid surface and, following impingement, the gas travels radially outwards from the impact point along the surface thereby dragging the liquid into motion and setting up a recirculation flow within the bulk (see Figure 1).

Three different modes of surface deformation have been identified: dimpling; splashing; and penetrating, dependent on the nozzle clearance, the jet momentum and the liquid properties (Molloy, 1970: see Figure 2). The modes differ in their free surface characteristics, degree of energy transfer from the jet to the liquid bath, and hence also bath mixing. Splashing and penetrating are both common in industrial situations, and while a significant volume of work has been published on the splashing mode, very little has been reported on the penetrating mode due to the complex nature of the gas and liquid flows.

The aim of this study is to model a gas jet impinging vertically onto a liquid bath using the computational fluid dynamics package CFX-F3D. In particular, to investigate all three modes of surface deformation (dimpling, splashing and penetrating) and to compare the results with the available experimental and theoretical data from the literature.

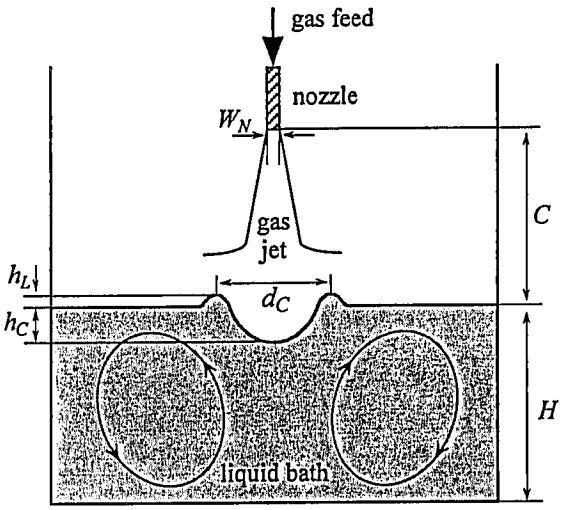

Figure 1: *Plane gas jet impinging vertically onto a liquid bath*

2.0 PREVIOUS WORK

Since the early 1960's a number of studies on gas jets impinging vertically onto a liquid surface have been reported in the literature. The focus has typically been on the characteristics of the free liquid surface, and to a lesser degree, the bulk liquid flow. An outline of the principal results from this literature is presented below.

2.1 Free Liquid Surface

A gas jet impinging vertically onto a liquid surface causes a depression to form on the free surface. The characteristics of this depression are primarily dependent on the jet momentum, the nozzle clearance and the liquid properties (Wakelin, 1966). The three modes of surface deformation which have been identified (dimpling; splashing; and penetrating) are shown in Figure 2 (Molloy, 1970). A majority of the literature has focussed on splashing due to its industrial importance. In spite of its industrial relevance, penetrating has received little attention due to the complexity of the unsteady, asymmetric gas and liquid flow fields.

Dimpling is observed for low jet momentums or high nozzle clearances. This mode is characterised by only a slight depression of the liquid surface (Figure 2a). As the jet momentum is increased or the nozzle clearance decreased, the depression depth increases until a point is reached where splashes, originating from the edge of the depression, start to be thrown radially outwards (Figure 2b). The volume of liquid splashed increases with an increase in the jet momentum or a decrease in the nozzle clearance up to a maximum value (Chatterjee and Bradshaw, 1972; Patjoshi *et al.*, 1982). Further increases in the jet momentum, or decreases in the nozzle clearance result in much deeper jet penetration into the bath. This is accompanied by a reduction in the amount of outwardly directed splash as the liquid is now thrown predominantly upwards and radially inwards (Figure 2c). The depression oscillates significantly in size, shape, and position producing a highly complex, asymmetric, overall flow pattern (Molloy, 1970).

Several workers have proposed similar theories to predict the depression dimensions applicable for both the dimpling and the splashing modes. As a result, the depression depth and width can be predicted based on an assumed depression shape (typically parabolic). An outline of this theory is presented in the following section. No theory has been developed for the depression formed in the penetrating mode due to the highly complex and unsteady nature of both the gas and liquid flows. In addition, correlations have been developed to describe the conditions at which the mode changes from dimpling to splashing, and from splashing to penetrating; these are discussed in the following section.

2.3 Liquid Flow Field

Following impingement the jet travels along the free liquid surface for some distance, thereby dragging the bulk liquid phase into motion. This radially outward flow is deflected at the tank walls and returns to the centre of the tank thereby producing a torodial vortex in the liquid phase (see Figure 1).

The characteristics of the induced liquid flow depend on the nature of the depression, with each mode producing a different amount of

energy transfer from the jet to the bath. At low jet momentums or large nozzle clearances, *i.e.* for the dimpling mode, the turbulent energies in the bulk liquid are small, and the impinging gas jet is a poor method of agitating the liquid. However, the rate of liquid mixing increases with both increasing jet momentum and decreasing nozzle clearance (Wakelin, 1966; Szekely and Asai, 1974).

Szekely and Asai (1974) and Zhang *et al.* (1985) propose similar numerical models to describe the bulk liquid flow. The models are based on solving the Navier-Stokes equations, and are applicable for the dimpling and splashing modes. The results presented by these workers show satisfactory agreement with experimental observations (Wakelin, 1966).

3.0 THEORY

3.1 Gas Flow Field

The decay in the centreline gas jet velocity, U_{CL}, with axial distance downstream of the nozzle exit, z, for a free turbulent plane jet is given by (Banks and Chandrasekhara, 1963):

$$\frac{U_{CL}(z)}{U_N} = K\sqrt{\frac{W_N}{z}} \qquad (1)$$

where U_N is the jet velocity at the nozzle exit, W_N is the nozzle width (see Figure 1) and K is a constant (a function of the jet Reynolds number and typically attains a value of approximately 2.5). Eq.(1) has been found to apply from beyond the potential core, up to close to the liquid surface for shallow cavities, *i.e.* for the dimpling and splashing modes.

3.2 Free Liquid Surface

An expression for the depth of the depression, h_C, formed on the free liquid surface by a vertically impinging plane gas jet can be found from a stagnation pressure analysis along the jet centreline. Banks and Chandrasekhara (1963), Turkdogan (1966), Wakelin (1966), Cheslak *et al.* (1969) and Chatterjee and Bradshaw (1972) have all proposed similar theories for the depression depth with the overall result:

$$\frac{h_C}{C}\left(1+\frac{h_C}{C}\right) = \frac{K^2}{2}\frac{M}{\rho_L g L_N C^2} \qquad (2)$$

where C is the nozzle clearance, M is the jet momentum and L_N is the nozzle length. The principal assumptions in the derivation of eq.(2) are that the effects of surface tension can be neglected and that the gas jet has negligible vertical momentum following impingement, *i.e.* the analysis is limited to shallow cavities. Nevertheless, eq.(2) has been found to give good agreement with experimental data within the dimpling and splashing modes.

Based on the assumption that the cavity is parabolic, an expression for the depression width, d_C, formed by a plane jet can be found by equating the weight of liquid displaced to the change in vertical jet momentum, giving:

$$\frac{d_C}{C} = \frac{6(1+\alpha)}{K^2}\left(1+\frac{h_C}{C}\right) \qquad (3)$$

where α is a function of the depression slope where the jet separates. This parameter can attain values of between 0 and 1: $\alpha = 0$ corresponds to very shallow cavities where the jet flow is approximately horizontal following impingement, while $\alpha = 1$ corresponds to deep cavities, where the gas flow tends to vertical following impingement (Banks and Chandrasekhara, 1963).

3.3 Transition from Dimpling to Splashing

Chatterjee and Bradshaw (1972) and Patjoshi *et al.* (1982) report that the transition from dimpling to splashing occurs at a critical depression depth, h_{DS}, which is almost solely dependent on the liquid properties. For a circular jet the following semi-empirical correlation is proposed:

$$\left(\frac{g\rho_L}{\sigma}\right)^{0.5} h_{DS} = \alpha_1 + \alpha_2 \log\left(\frac{g\mu_L^4}{\rho_L \sigma^3}\right) \qquad (4)$$

where α_1 and α_2 are constants. For $g\mu_L^4/(\rho_L\sigma^3) = 10^{-14} - 10^3$, $\alpha_1 = 11.3$ and $\alpha_2 = 0.53$. These values correspond to a

critical depression depth of around 15 mm for and air-water system.

In contrast, Molloy (1970) suggest that it is the jet velocity in the vicinity of the free surface which determines the mode of deformation. It is proposed that the transition from dimpling to splashing occurs when the jet velocity at the original liquid surface level exceeds 15 m s^{-1} for a circular jet in an air-water system. Based on the range of experimental conditions over which this criteria was developed, it also results in a critical depression depth of approximately 15 mm.

The use of the jet velocity in the vicinity of the free surface to correlate the transition from one mode to another is in agreement with the experimental observations of Wakelin (1966). This investigator concludes that it is the jet velocity in the impingement area which is the main factor influencing the break-up of the liquid surface.

3.4 Transition from Splashing to Penetrating

The transition from the splashing to penetrating mode is postulated by Molloy (1970) to occur when the jet velocity at the original liquid surface level exceeds 75 m s^{-1}. This is again based on a circular jet in an air-water system.

4.0 CFX-F3D MODELLING

A transient two-dimensional slice model of a vertical plane gas jet impinging onto a liquid bath has been developed using the computational fluid dynamics package CFX-F3D. The basic jet and bath geometries are similar to those employed by Chatterjee and Bradshaw (1972) and Wakelin (1966). Three different simulations were conducted, as summarised in Table 1, which aimed to cover the three different modes of depression described earlier and shown in Figure 2. These conditions were selected based on the mode transition correlations presented in §3.3 and §3.4, where it has been assumed that the correlations apply equally to circular and plane jets. In summary, the nozzle clearance was kept constant throughout, and the jet momentum was gradually increased to cover each mode.

The computational grid consisted of a 150 × 150 rectangular mesh; the smallest cell sizes were located in the axis of symmetry region, immediately downstream of the nozzle exit plane and in the proximity of the free surface. The use of a finer grid (200 × 200 cells) had a negligible effect on the resulting gas and liquid flows. The simulations included the surface sharpening algorithm, which forms part of the CFX-F3D software, and adapts the volume fraction equations in the proximity of the free surface to minimise smearing of the interface due to numerical diffusion. The gas jet exits the nozzle with a fully developed pipe flow profile, and the k-ε turbulence model has been employed, as used successfully by Zhang *et al.* (1985). The gas exits the system through pressure boundaries positioned well above the nozzle exit plane.

The CFX-F3D software was tested for this two-phase geometry by Forrester and Evans (1996) who successfully modelled a test case reported by Zhang *et al.* (1985).

5.0 RESULTS AND DISCUSSION

5.1 Depression Characteristics

The shape of the depression formed in each Run is presented in Figure 3. The similarity in the shapes to those presented in Figure 2 confirm the suitability of the criteria given in §3.3 and §3.4 to determine the jet velocity for each mode.

The dimpling mode (Run 1) is characterised by the steady state formation of a shallow depression, with the gas flow close to horizontal following impingement.

The splashing mode (Run 2) is characterised by a deeper (and wider) depression, however the gas flow still remains close to horizontal following impingement. A steady state solution could not be achieved for this system with the periodic formation of ripples around the lip of the depression which proceeded to moved radially outwards while reducing in height. This was combined with a slight vertical oscillation in the depression depth.

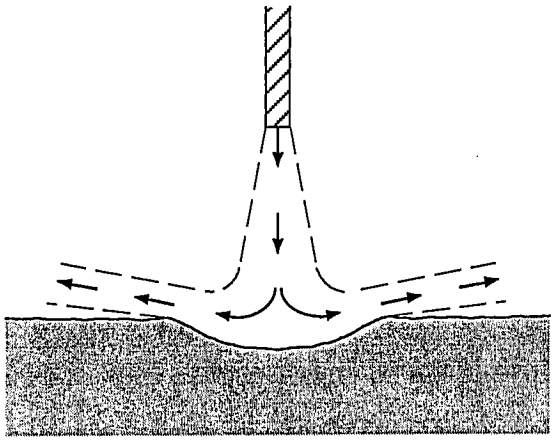

(a) dimpling

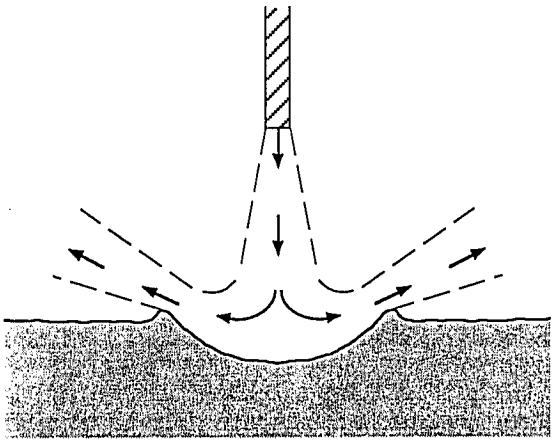

(b) splashing

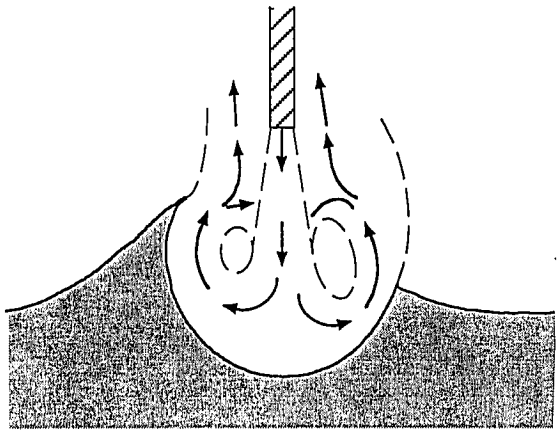

(c) penetrating

Figure 2: *Modes of surface deformation* (Molloy, 1970)

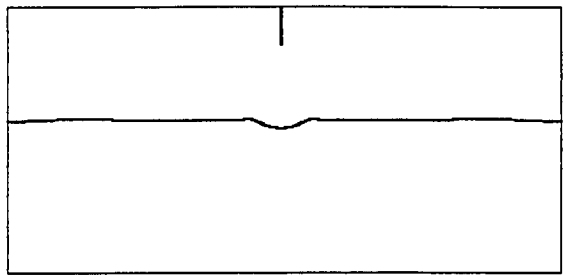

(a) Run 1

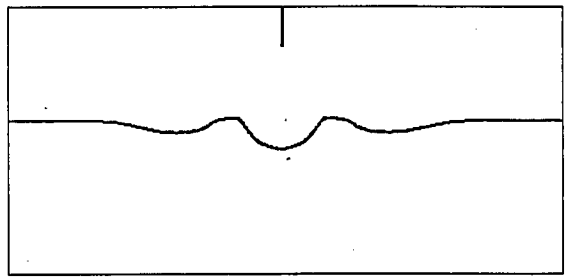

(b) Run 2

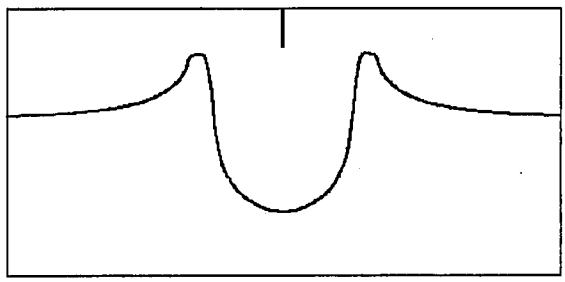

(c) Run 3

Figure 3: *CFX-F3D cavity shape results*

As a first approximation in the CFX-F3D work, the liquid phase was assumed to be continuous, and therefore the splashing which occurs under real conditions has not been modelled.

The penetrating mode (Run 3) is characterised by a significant increase in the cavity depth such that the walls are close to vertical. The lip, marking the edge of the cavity, moves well above the original liquid level, and, similarly to the splashing mode, waves formed at the lip and move radially outwards. There is also significant vertical oscillation in the cavity depth. The CFX-F3D solution remains symmetrical, in contrast to the real situation, due to the symmetry of the initial conditions and boundary conditions applied.

5.2 Centreline Gas Velocity

The decay in the centreline gas jet velocity for each Run is shown in Figure 4. In addition to the CFX-F3D results, the theory for the expansion of a free turbulent plane jet, given by eq.(1), is also presented. The results indicate that for all three simulations there is a zone of good agreement between the CFX-F3D results and the theory downstream of the potential core region , *i.e.* for $z/W_N > \sim 6$.

In both the dimpling and splashing modes where the surface depression is not very deep and the sides not very steep (such that the gas flow is close to horizontal following impingement), then the zone of good agreement extends up to quite close to the free liquid surface; to around $z/W_N = \sim 30$ in both cases, before the velocity drops off rapidly to zero as the stagnation point on the free surface is approached (which occurs at $z/W_N = \sim 43$ in Run 1 and $z/W_N = \sim 51$ in Run 2).

In the penetrating mode the zone of good agreement is shorter than in the previous two runs. This is due to the increased cavity depth, with correspondingly steeper walls and a lip which rises to a significant height above the original liquid level. However, the deviation from the free jet expansion theory is not very significant until approximately the same distance, *i.e.* $z/W_N = \sim 30$. The influence of the cavity walls on the jet expansion characteristics is likely to be small due to their distance from the jet axis.

The best fit value of the constant K in the free jet expansion equation was found to be 2.6 for all three runs. This is in good agreement with values typically quoted in the literature, *e.g.* Banks and Chandrasekhara (1963).

5.3 Depression Dimensions

The cavity dimensions predicted by the theory given in §3 are compared with the CFX-F3D results in Table 2. The values of the depression depth, lip height and depression width are presented.

Considering initially the values of the cavity depth, there is good agreement between the CFX-F3D results and the theory for both the dimpling and splashing modes (for which the theory was developed). However, eq.(2) overpredicts the cavity depth for the penetrating mode; the steep cavity walls result in the gas jet leaving the depression with a significant vertical momentum.

The CFX-F3D results indicate that the lip height (defined in Figure 1) in both the dimpling and splashing modes is small, typically around 20 percent of the cavity depth. In the penetrating mode the lip height is much greater, and is now of the same order as the cavity depth. There is no theory for this parameter with which to compare the results of this study.

The depression width results again show good agreement between the theoretical values and the CFX-F3D results in both the dimpling and splashing modes. This indicates that the assumption of a parabolic cavity and setting $\alpha = 0$ are reasonable assumptions in each of these modes. The theoretical value for the cavity width in the penetrating mode also gives good agreement with the CFX-F3D result. However, this comparison is not appropriate: as noted above the theoretical value is based on a cavity width significantly greater than that observed in the CFX-F3D work; and it is unlikely that setting $\alpha = 0$ is acceptable due to the steepness of the cavity walls. A more appropriate theoretical value would be achieved by applying the CFX-F3D

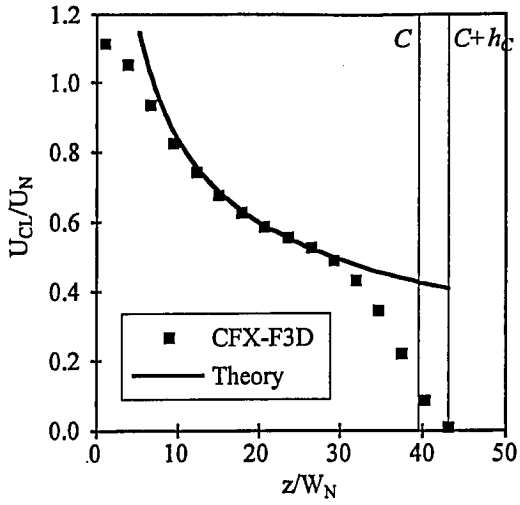

(a) Run 1

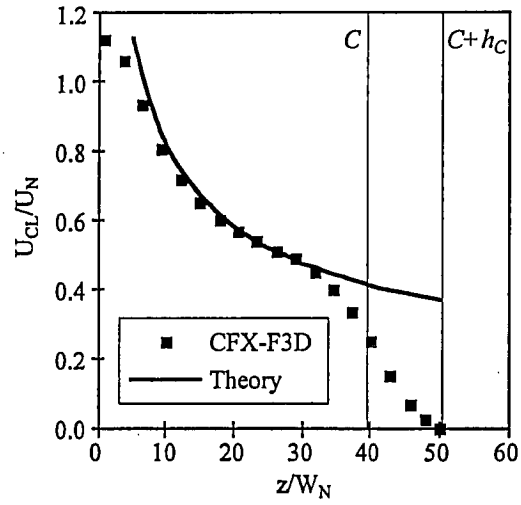

(b) Run 2

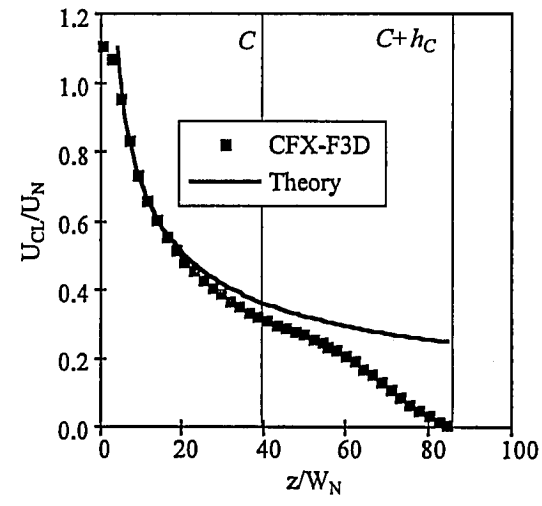

(c) Run 3

Figure 4: *Gas jet centreline velocity profiles*

value of the cavity depth and $\alpha = 1$ in eq.(3), giving a cavity width of 385 mm compared to the CFX-F3D value of 222 mm. This suggests that the assumption of a parabolic cavity, on which eq.(3) is based, is not acceptable for the penetrating mode.

6.0 CONCLUSIONS

A plane turbulent gas jet impinging onto a free liquid surface has been successfully modelled using the computational fluid dynamics package CFX-F3D. Three simulations are presented, based on a fixed geometry and increasing gas jet velocity, which correspond to the three different modes of surface deformation reported in the literature, *i.e.* dimpling, splashing and penetrating.

At low gas jet velocities a shallow cavity is formed on the liquid surface the dimensions of which can be well predicted based on the assumptions that the cavity is parabolic in shape, the gas flow prior to impingement can be modelled as a free turbulent jet, and the gas flow following impingement is entirely horizontal. As the gas jet velocity is increased the cavity becomes deeper and wider with the walls tending to vertical, and the lip marking the outer boundary of the cavity rising significantly above the original liquid level. The cavity becomes unsteady with oscillation in both the depth and width and ripples form at the lip before moving radially outwards.

Finally, the next stages of this work include analyse of the period of oscillation observed in the cavity depth, the frequency of ripple formation, and to relax the liquid continuum assumption such that the formation of droplets observed industrially can be included in the CFX-F3D simulations.

REFERENCES

Banks, R.B. and Chandrasekhara, D.V., 1963, Experimental investigation of the penetration of a high-velocity gas jet through a liquid surface, *J. Fluid Mech.*, **15**, 13 – 34.

Chatterjee, A. and Bradshaw, A.V., 1972, Break-up of a liquid surface by an impinging gas jet, J. *Iron Steel Inst.*, March, pp.179 – 187.

Cheslak, F.R., Nicholls, J.A. and Sichel, M., 1969, Cavities formed on liquid surfaces by impinging gaseous jets, *J. Fluid Mech.*, 36, pp.55 – 63.

Forrester, S.E. and Evans, G.M., 1996, Air jets impinging onto unconfined and confined liquid pools, paper presented at the *3rd CFX Int. Users Conf.*, London, U.K.

Molloy, N.A., 1970, Impinging jet flow in a two-phase system: The basic flow pattern, J. Iron Steel Inst., October, pp.943 – 950.

Szekely, J. and Asai, S., 1974, Turbulent fluid flow phenomena in metals processing operations: mathematical description of the fluid flow field in a bath caused by an impinging gas jet, *Metall. Trans.*, **5**, 463 – 467.

Turkdogan, E.T., 1966, Fluid dynamics of gas jets impinging on surface of liquids, *Chem. Engng Sci.*, 21, pp.1133 – 1144.

Wakelin, D.H., 1966, The interaction between gas jets and the surface of liquids including molten metals, *Ph.D. Thesis*, University of London, U.K.

Zhang, J., Du, S. and Wei, S., 1985, Flow field in bath agitated by symmetrically placed impinging gas jet and submerged gas stream, *Ironmaking and Steelmaking*, **12**, 249 – 255.

Table 1: *Summary of the simulation conditions*

run	mode	W_N (mm)	L_N (mm)	D_C (mm)	C (mm)	H (mm)	M (kg m s^{-1})	U_N (m s^{-1})	$U_{CL}(C)$ (m s^{-1})
1	dimpling	2.53	2.0	730	100	200	0.005	28.8	12
2	splashing	2.53	2.0	730	100	200	0.02	58.0	24
3	penetrating	2.53	2.0	730	100	200	0.25	203	84

Table 2: *Summary of the depression shape results*

run	CFX-F3D			Theory				
	h_C (mm)	h_L (mm)	d_C (mm)	h_C (mm)	h_L (mm)	d_C (mm)	K (-)	α (-)
1	10	2	86	8.5	0	96	2.6	0
2	29	6	102	28	0	114	2.6	0
3	117	90	222	164	0	236	2.6	0